All-aqueous Synthesis of Fibrillated Protein Microcapsules for Membrane-bounded Culture of Tumor Spheroids

Yue Wei[1, 2], Zhixiang Cai[3*], Ting Yang[1], Shi Yang[1], Xiuli Xu[1], Han Yu[1], Rui Zan[5], Hongbin Zhang[3], Zhou Liu[2], Changkun Liu[2], Tiantian Kong[4*], Yang Song[1*]

1. State Key Laboratory of Metal Matrix Composites, School of Material Science and Engineering, Shanghai Jiao Tong University, Shanghai 200240, China.
2. College of Chemistry and Environmental Engineering, Shenzhen University, Guangdong 518071, China.
3. School of Chemistry and Chemical Engineering, Shanghai Jiao Tong University, Shanghai 200240, China.
4. School of Biomedical Engineering, Health Science Center, Shenzhen University, Guangdong 518071, China.
5. Shanghai Engineering Research Center of Biliary Tract Minimal Invasive Surgery and Materials, Shanghai, China.

Correspondence addressed to Dr. Yang Song. Email: nanosurface@sjtu.edu.cn

Abstract

Water-in-water (W/W) emulsion provides cytocompatible compartments for cell encapsulation and 3D printing of tissues. Formation of semi-permeable membrane at the W/W interface is critical to entrapment of cells in the droplet phase and supply of nutrients from the continuous phase. However, the adsorption of colloidal particles at the W/W interface is dynamic and reversible, which represents an inherent limitation for fabrication of mechanically robust cell-laden microcapsules. Here we demonstrate the preparation of thin, inflatable and semi-permeable microcapsules by using clusters of protein fibrils as building blocks and control their assembly at W/W interface. These fibril clusters are prepared by cross-linking lysozyme fibrils with multi-arm polyethylene glycol (PEG) through click chemistry. Compared to linear-structured fibrils, fibril clusters can strongly adsorb at W/W interface, and they packed into an interconnected meshwork to stabilize W/W emulsion. Moreover, when fibril clusters are complexed with calcium alginate, the hybrid microcapsules can bear a high osmotic gradient of 60 mOsm/Kg induced by dextran (Mw=500,000), and their surface area expand by over 100% without rupture. This all-aqueous biomaterial synthesis approach allows fabrication of mechanically robust capsules for long-time culture of SGC-996 tumor spheroids, with great potentials to be used in anti-tumor drug-screening and tissue transplantation.

Keywords: water-in-water emulsion, fibril cluster, protein microcapsules, semi-permeability, tumor spheroids.

Introduction

Water-in-water (W/W) emulsions are droplets derived from spontaneous liquid-liquid phase separation of a macromolecular solution.[1] In biology, membraneless organelles and nuclear bodies are representative W/W emulsions,[2, 3] and they serve as liquid chambers to compartmentalize biomolecules and coordinate their cellular functions. Bioactive molecules and cells largely preserve their native structures and biological functions in the all-aqueous environment.[4, 5] Consequently, W/W emulsions are more advantageous over traditional water/oil emulsions for processing of biomolecules,[1, 4, 6, 7] and they are increasingly exploited as liquid scaffolding for patterning of cells, culture of organoids and printing of tissues.[8-13] W/W interface are highly permeable to oxygen, nutrients, metabolic waste, and even living cells. To confine cells within the predesigned liquid chambers or patterns,[14] hydrogel precursors are frequently mixed with the cell-laden droplet phase, and the subsequent gelation of the precursor immobilize cells into the hydrogel. However, the hydrogel matrix, if not degraded timely, will retard the perfusion of nutrients[15] and fusion of cell aggregates for tissue culture.[16]

An alternative hydrogel-free cell-culture strategy is to building a semi-permeable membrane at the W/W interface that blocks the undesired migration of cells. Nutrients and metabolic wastes could still diffuse across the semi-permeable membrane to support long term culture of cells, spheroids and organoids. To form semi-permeable membranes, polymers and colloidal particles can be used as building blocks for membrane formation at the W/W interface. However, interfacial tension of W/W

emulsion is several orders of magnitude lower than water/oil emulsion,[1, 17] leading to the weak adsorption energy and low coverage ratio of colloidal particles at the W/W interface.[18] Consequently, microcapsules and membranes formed at the W/W interface often yields low mechanical strength.[17, 19] To optimize the colloidal adsorption and their stacking at the W/W interface, colloids with different shapes and surface wetting properties have been explored for stabilization of W/W emulsions.[17, 20-24] However, it is difficult to achieve simultaneously suitable mechanical strength and membrane permeability for tissue culture.[25] The feasibility to fabricate robust and semi-permeable capsules at the W/W interface will provide new solutions to control spatial configuration of tissues, without sacrificing their interior permeability.

Protein nanofibrils are one-dimensional nanomaterials with excellent mechanical strength and cytocompatibility.[17, 26] Like natural extracellular matrix, synthesized protein nanofibrils can be organized into 3D networks that promote cell adhesion, proliferation and differentiation, revealing irreplaceable implications in tissue engineering.[27-29] We have previously reported an all-aqueous approach to fabricate robust 'fibrillosomes' by cross-linking lysozyme fibrils at the W/W interface, forming two-dimensional multilayer fibril networks.[17] However, fibrillosomes are only stable in acidic solutions (pH= 2-4), and they collapse into solid precipitates in pH-neutral solutions. To further develop a nanofibrils-coated droplet chamber for tissue culture, here we synthesized multi-arm PEG cross-linked fibril clusters as new building blocks for stabilization of W/W emulsions in pH-neutral solution. These fibril clusters are subsequently complexed with alginate to prepare robust membrane at the W/W

interface, yielding thin-shelled, inflatable and semi-permeable capsules that support long-term culture of large tumor spheroids over 200 μm.

Preparation and characterization of fibril clusters

Lysozyme fibrils were prepared by dissolving 2% (w/v) lysozyme monomers (from hen egg white) in a strong acidic solution (206 mM HCl and 200 mM NaCl), followed by vigorous stirring at a shear rate of 8 rad s^{-1} at 70 ℃. After incubation for 65 hours, the resulting fibrils have dimensions of 500-1000 nm in length, and 15-20 nm in thickness.[17] After suspended in a mixture of 7% PEG and 3% dextran, the fibrils (0.05-0.2 wt%) can be adsorbed at the W/W interface and stabilize W/W emulsion droplets at pH= 2-4. When the medium pH is adjusted to 7, the β-sheet structure of lysozyme fibrils become unstable, and they partition into the dextran-rich droplet phase (Fig.S1). According to the Bancroft's rule, an effective surfactant of emulsion should have a higher affinity in the continuous phase than the droplet phase, we thus grafted polyethylene glycol (PEG) to the lysozyme fibrils and enhances their affinity to the PEG-rich continuous phase. Experimentally, lysozyme fibrils were first decorated with furan moieties, and the furan modified fibrils were further reacted with maleimide-decorated multi-arm-PEG (Mw: 10 kDa) through Diels-Alder (D-A) click chemistry (see schematic Fig. 1a).

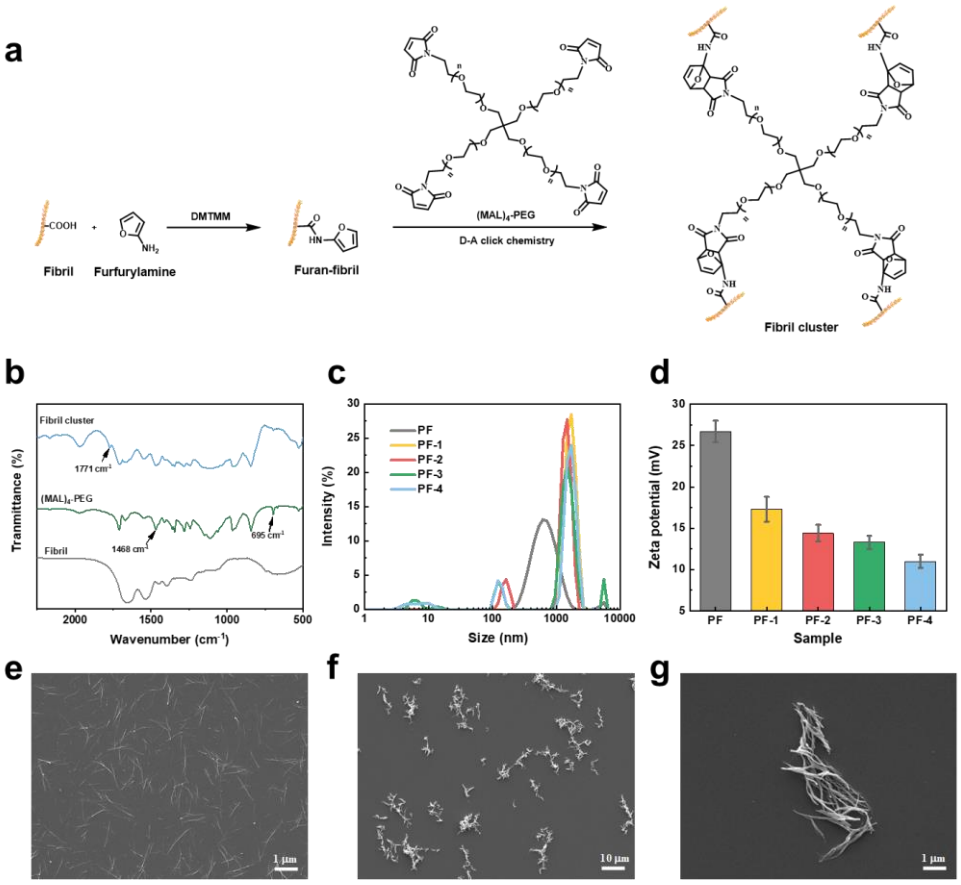

Fig. 1 (a) Schematics on the synthesis of furan-decorated fibril and PEGylated fibril clusters through D-A click chemistry. (b) FT-IR spectra of native fibril, $(MAL)_4$-PEG, and fibril cluster. (c) Size distribution and (d) zeta potential of native fibril and fibril clusters. (e-g) Morphology of native fibril and fibril clusters observed in SEM.

Table 1 Mass ratios of multi-arm PEG to lysozyme fibrils in different fibril clusters.

Sample	PF-1	PF-2	PF-3	PF-4
Nominal weight ratios of fibrils to PEG	1:12.5	1:25	1:37.5	1:50
PEG weight fraction (%)	49 ± 9	66 ± 6	80 ± 2	86 ± 2

According to the FT-IR spectrum in Fig.1b, $(MAL)_4$-PEG exhibits characteristic absorption peak at 695 cm^{-1} and 1468 cm^{-1}, which correspond to the bending motion of ═C−H and C═C bonds in the maleimide.[30, 31] After the fibrils are modified with $(MAL)_4$-PEG, an absorption peak appears at 1771 cm^{-1}, in accordance with C═C stretching vibrations of the D-A adduct.[30] The results confirm the successful connection of multi-arm PEG with fibrils. By varying the mass ratios of multi-arm PEG to lysozyme fibrils (see Table 1) in the reaction mixture, we obtain a serial of PEGylated fibril clusters with increasing PEG fractions from 49 wt% to 86 wt.%, named as sample PF-1, PF-2, PF-3, PF-4 (see specific compositions in table 1). As the PEG fraction in the fibril cluster increases, the hydrodynamic diameter of the PEGylated fibril clusters increases from 1 micrometer to 10 micrometers, as evidenced by both dynamic light scattering (DLS) measurement (Fig.1c) and scanning electron microscopy (SEM) observation. Due to the shielding of charge induced by 4-arm PEG moiety,[32, 33] the zeta potential of fibril decreases from +27 mV to +11 mV (Fig.1d). SEM observation reveals the number of fibrils in each cluster typically varies from 6 to 40 pieces, Fig.1e-g).

Stabilization of W/W emulsion by fibril clusters

Next, we investigated the interfacial stability of W/W emulsions after addition of PEGylated fibril clusters (Fig.2a). Fibril clusters with different PEG fractions were synthesized and stained by thioflavin T and suspended in an emulsion mixture of 3% dextran / 7% PEG / 90% H_2O at the concentration of 0.05%-0.15% (w/v, counted by protein fibrils). After vortex mixing, the fibril cluster-stabilized emulsion droplets were

observed using fluorescence microscopy. With an increasing PEG fraction in the fibril cluster, more fibrils were observed to translocate from the dextran-rich droplet phase to the W/W interface, resulting in a higher density of stable W/W droplets with decreasing droplet size (Fig.2b and S2). The observation suggests that the 4-arm PEG enhances the partitioning affinity of fibril cluster to the continuous phase and W/W interface, thereby improves the emulsion stability. By fixing the PEG fraction (at PF-4) and increasing the concentration of fibril cluster, the average diameter of the W/W emulsion also decreases, suggesting that the stabilized total interfacial area of the emulsion mixture increases with the concentration of fibril cluster. (Fig. 2c).

Molecular weight of 4-arm PEG in the fibril cluster also influence the emulsion stability. In our experiment, fibril cluster with a high PEG molecular weight (Mw: 2.5k × 4 = 10 kDa) exhibits much stronger capability to stabilize dextran-in-PEG emulsion, compared to that with relatively low PEG molecular weight (Mw: 2 kDa and 5 kDa) (Fig. 2d). This observation can be explained by the Bancroft's rule that packing parameter of surfactants determines the emulsion type and stability. When fibril clusters are adsorbed at the W/W interface, the 4-arm PEG moiety has a high affinity to the PEG-rich continuous phase, while the fibril 'tails' tend to stay in the dextran-rich droplet phase. The volume ratios of the 4-arm PEG moiety to the fibril can be adjusted by changing the molecular weight of the PEG or their mass ratios. If the volume of the PEG moiety is larger than that of the fibril tail, the assembly of fibril cluster at W/W interface should maintain a positive curvature and better stabilize the dextran-in-PEG emulsion.

To further understand how the molecular structure of fibril cluster contributes to the improved emulsion stability, we also compared the W/W emulsion stabilized by PEGylated single fibrils (Fig. 2e) and fibril clusters (Fig. 2f). PEGlated single fibrils are synthesized by decorating maleimide-(PEG)-OCH_3 on the surface of fibrils, yielding "comb-like" fibril structure. In contrast, the 4-arm PEG cross-linked fibril clusters have "mesh-like" structure. When the two kinds of fibril structures are separately suspended into the dextran-PEG-H_2O system, both the "comb-like" fibrils and "mesh-like" fibril cluster can locate at the W/W interface; however, the "comb-like" fibrils are unable to stabilize W/W emulsions as robust as fibril clusters. The superior emulsion stability after addition of "mesh-like" fibril clusters can be explained by their higher adsorption energy to the W/W interface, relative to the "comb-like" single fibrils. Assuming all fibrils are lying at the W/W interface, the adsorption energy of single fibril to the W/W interface can be estimated from $\Delta G_{fib} = 2R\gamma_{W/W}L(\sin\theta + \pi\cos\theta - \theta\cos\theta)$,[17, 34] where θ is the wetting angle of fibrils at the W/W interface, L and R represent the length and radius of fibrils, and $\gamma_{W/W}$ is the interfacial tension between the two immiscible aqueous phases. When fibrils are cross-linked into clusters by multi-arm PEG, the adsorption energy becomes $\Delta G_{cls} = n\Delta G_{fib}$, where n represents the average number of fibrils ($n \approx 15$) in each cluster. Note that the high flexibility of the multi-arm PEG is critical to keep fibrils lying on the W/W interface and thus maximize their contact area with the W/W interface. With similar PEG fraction in the "comb-like" fibrils and "mesh-like" fibril clusters, the wetting angle, θ, is almost unchanged, so the adsorption energy of fibril cluster at the

W/W interface is about ~15 folds higher than that of single fibrils. This model explains the exceptional high capability of fibril cluster to stabilize the W/W emulsions. Besides, compared to the "comb-like" fibrils, the "mesh-like" fibril clusters could entangle with each other, forming interconnected colloidal networks to enhance the stability of W/W emulsions.

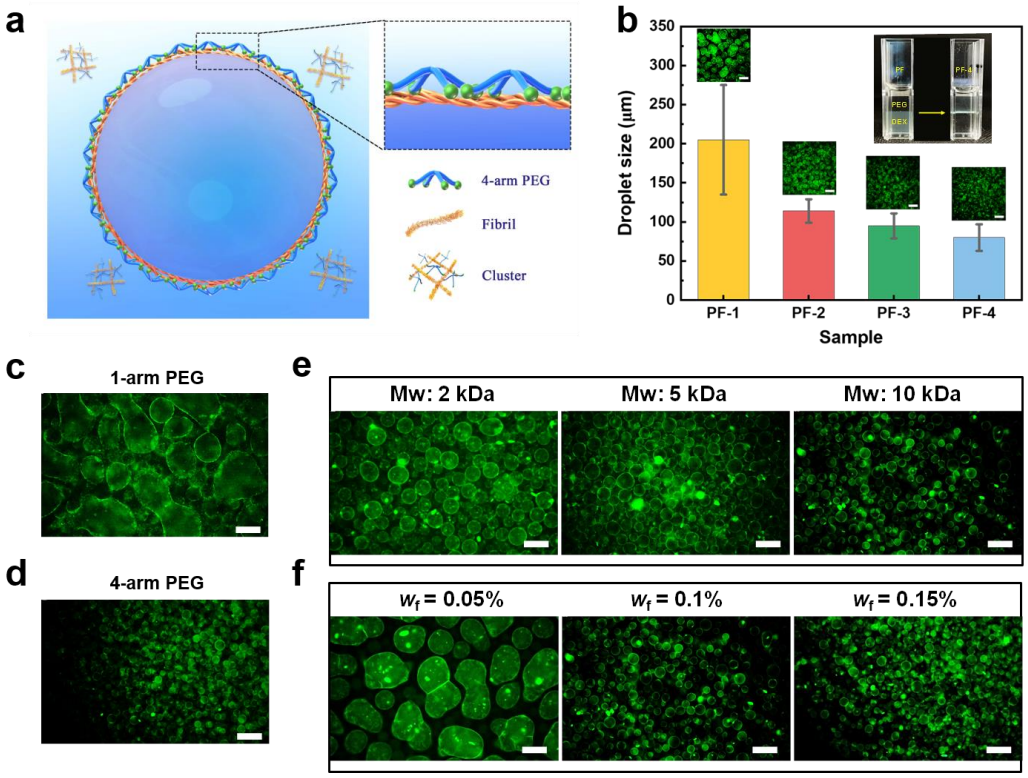

Fig. 2 (a) Schematic illustration of partitioning and interfacial packing of fibril clusters at the W/W interface. (b) The fluorescence images and the average size of emulsion droplets stabilized by fibril cluster with different PEG fractions. The inset shows the partitioning behaviors of ThT-labelled native fibrils and fibril clusters (PF-4) at pH=7. (c) Concentration-dependent stabilization of W/W emulsion by fibril clusters. (d) Fluorescence microscopy images of W/W emulsion stabilized by fibril clusters with different molecular weight of PEG crosslinkers. (e) Fluorescence microscopy images of emulsion droplets stabilized by (e) 1-arm PEG modified fibrils and (f) 4-arm PEG cross-

linked fibril clusters, pH=7. Scale bars, 50 μm.

Fabrication of fibril cluster/alginate hybrid capsules

To strengthen the colloidal network of fibril clusters adsorbed at the W/W interface, we separately added 0.15% sodium alginate and 0.15% fibril clusters from the droplet and continuous phases, and generated W/W emulsion through electrospray. After the alginate-laden dextran-rich droplets are sprayed into the cluster-laden PEG-rich continuous phase, the anionic sodium alginate molecules are complexed with cationic fibril clusters through electrostatic attraction at the W/W interface. As sodium alginate molecules continuously diffuse across the W/W interface and react with fibril clusters, a core-shell structured capsules are formed, until the completed consumption of the sodium alginate in the droplet phase. By transferring the capsules into the calcium chloride solution, the fibril cluster/alginate complexes are solidified into microcapsules (Fig. 3a). SEM observation confirms that the capsules are intact, composed of multilayered fibrils on their surface (Fig.3b). These capsules with hollow chambers (Fig.3c) can maintain stable in cell-culture medium for over several months.

To confirm that both alginate and fibril clusters constitute the capsules, we conducted a dissolution test by separately degrading calcium alginate and fibril clusters in the capsules (Fig. 4). The hybrid capsules can be fully destroyed after soaking in 150mM sodium citrate solution (Fig. 4a), or cell culture medium supplemented with 0.25% trypsin-EDTA (Fig. 4b). With the rupture of capsules, macromolecules can

rapidly release into the surrounding aqueous environment, as shown by releasing FITC-dextran (Mw: 2 million) from these capsules. When the hybrid capsules are immersed in a diluted 0.125wt% trypsin-EDTA solution, the lifetime of capsule is extended by a few hours (Fig. S3). These observations suggest that the lifetime of capsules can be controlled by varying the enzyme activity in the surrounding aqueous environment.

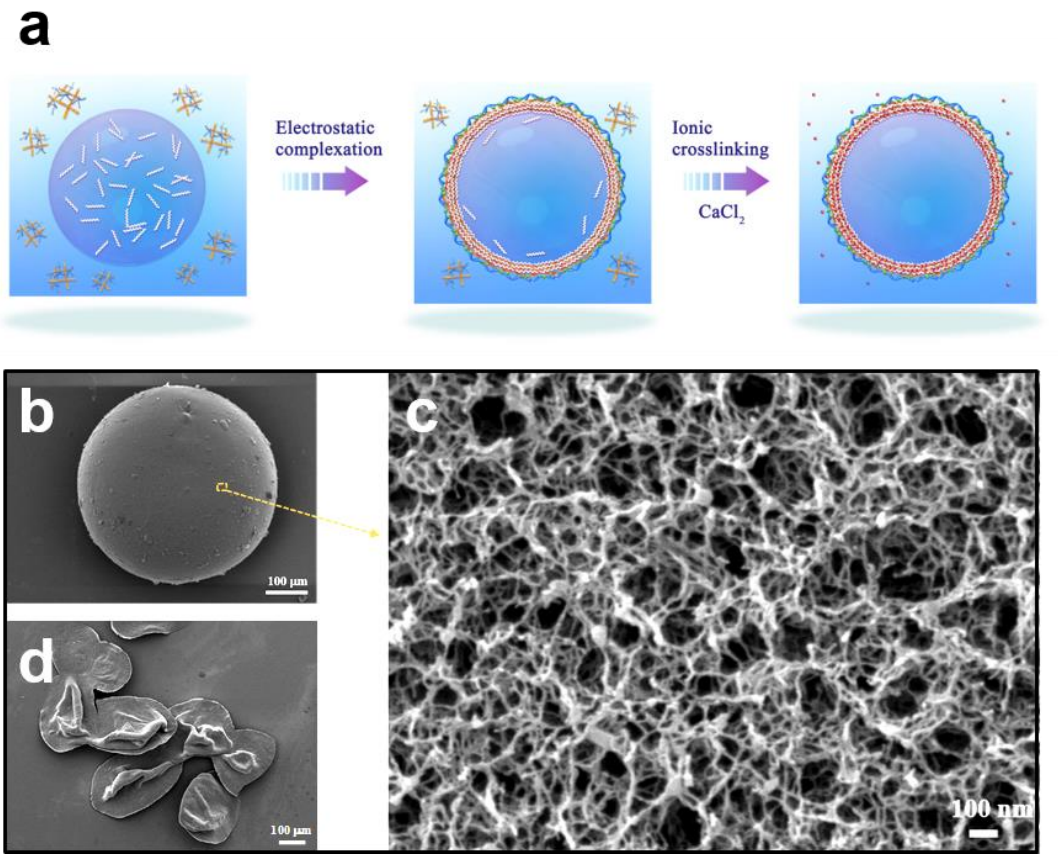

Fig. 3 (a) Schematics on the fabrication of the microcapsules based on the interfacial complexation between fibril clusters and alginate. (b,c) SEM images of the hybrid capsules dried in the liquid carbon dioxide at its super critical point. (d) SEM image of hybrid capsules dried in air.

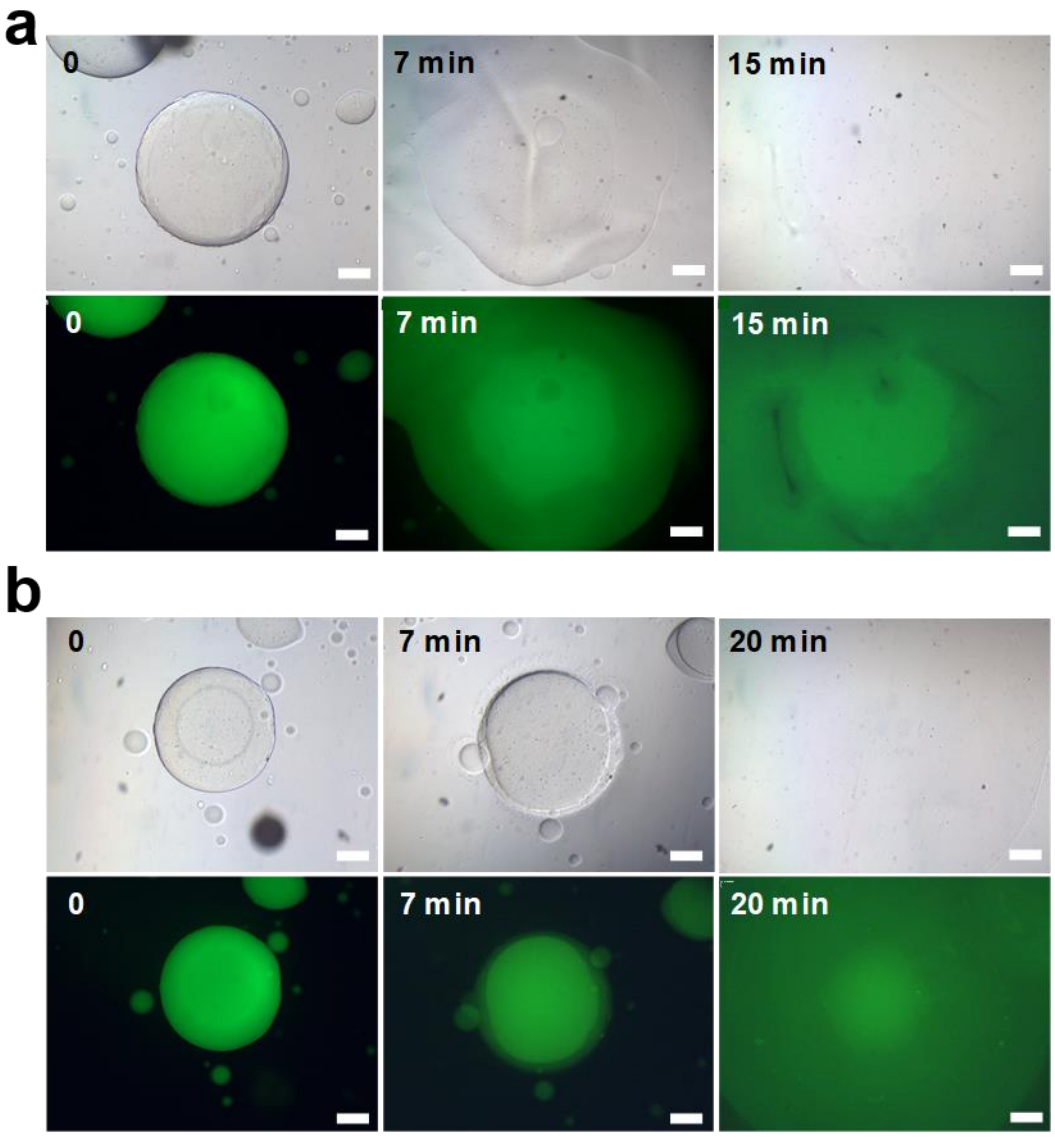

Fig. 4 Degradation of microcapsules by using enzymes or ionic chelators. (a) Rupture of microcapsules in sodium citrate (150 mM) and (b) trypsin-EDTA (0.25% w/v), and the release of FITC-dextran (Mw: 2 million Da) inside the capsules are shown by the corresponding fluorescence microscopy images. Scale bars: 200 μm.

Mechanical properties and permeability of capsules

The mechanical properties of the microcapsules were assessed by monitoring the

inflation of the capsules in hypotonic solutions of dextran. Experimentally, the droplet phase is dissolved with 15% dextran (Mw=500,000), and the external phase is replaced by dextran solutions with different concentrations (1%~15%, w/v). Due to the presence of concentration gradient of dextran, an osmotic pressure is introduced to the capsules and drive their slow inflation (Fig. 4a). When the concentration of dextran in the external phase is reduced to 1 wt%, a high osmotic pressure of about 60 mOsm/Kg is generated, and the capsules remain intact without rupture. The expansion ratio of surface area, η, defined by $\eta = \frac{S_1}{S_0} = (\frac{D_1}{D_0})^2$, is measured from the changes in the diameter of the capsules. To reflect the change in permeability due to the osmosis-induced inflation, two fluorescent dyes, FITC-dextran with different Mw (150 kDa and 2000 kDa, 0.1%) are separately added into the droplet phase at a low concentration of 0.05%. In absence of osmotic pressure, the FITC-dextran with Mw of 150 kDa can not penetrate through capsules. Upon a relatively large osmotic pressure (> 50 mOsm/Kg) is applied, the pore size of the capsule becomes large enough for diffusion of FITC-dextran. When the molecular weight of FITC-dextran is increased from 150 kDa to 2000 kDa, no leakage of the dye can be observed, even if an osmotic pressure of 60 mOsm/Kg is given. The change in the semi-permeability of the capsules suggests that the pore sizes increases with osmotic pressure. FITC-dextran with a molecular weight of 40 kDa can always penetrate through the capsules, regardless of the osmotic pressure applied. The observation suggests that the capsules should allow bidirectional diffusion of nutrients, and metabolic waste across the membrane.[8, 35]

Resistance of microcapsules against shear force is further characterized by suspending capsules in dextran solution and measured using a rotational rheometer. Firstly, dynamic frequency sweeps were conducted to probe the viscoelastic properties of the microcapsule suspensions, as is shown in Fig. 4b. The dextran solution is predominantly viscous ($G' < G''$), while the addition of microcapsules leads to increased moduli. Moreover, with an increase in the volume fraction of the capsules, an enhanced elasticity can be observed from the tan δ (= G''/G'). The steady shear viscosity measurements were conducted, as shown in Fig. 4c. While the dextran solution exhibits a typical Newtonian behaviour with a constant viscosity of ca. 0.1 Pa s, the capsule suspensions exhibit shear-thinning behaviours. The rigidity of the capsules and their aggregates contribute to the improved viscoelastic moduli and non-Newtonian behaviours, attributed to the dense fibril network structure in the capsules and the interactions among capsules. Moreover, comparing the steady shear viscosities η with the complex viscosity η^*, which was deduced from the dynamic frequency sweep test, the empirical Cox–Merz rule[36] stating $|\eta^*(\omega)| \cong |\eta(\dot{\gamma})|_{\dot{\gamma}=\omega}$ is not obeyed, with $\eta^* > \eta$ for the microcapsule suspensions. This discrepancy indicates that steady and oscillatory shear probe different states of the suspensions. The steady shear imposed on the suspensions can disrupt the cluster structure and the fibril network structure, and thus decreases their contribution to suspension viscosity.[37] By contrast, the oscillatory shear test has very weak destructive effects on the capsules' structure, and the rheology reflects more contribution of the capsules formed by fibril clusters.

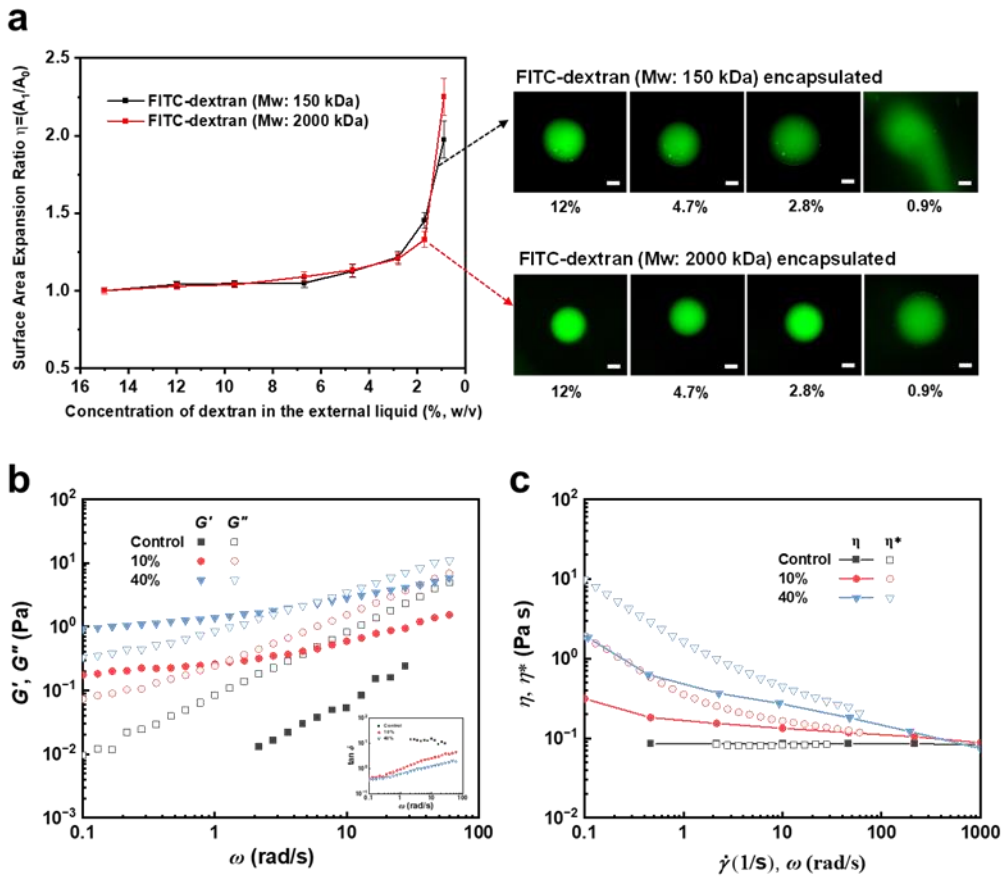

Fig. 5 (a) Change in surface area and membrane permeability as a function of osmotic gradients induced by dextran. 0.05% FITC-dextran with different Mw (150 and 2000 kDa) was preloaded in the capsules, and the release of FITC-dextran reveals the enlarged pore size after swelling of capsules. (b) Storage (G') and loss (G'') moduli for microcapsule suspensions with different volume fractions (φ =0, 10%, and 40%) as a function of frequency (ω). (c) Complex viscosity (η^*) and steady shear viscosity (η) as a function of frequency and shear rate, respectively. The control sample is 15% (w/v) dextran solution. The insets in b shows the variation of tan δ with frequency.

Cell Encapsulation and Spheroids Culture in Microcapsules

This all-aqueous capsule-synthesis approach offer good opportunities to culture

cells in membrane-supported liquid compartments.[38] By mixing cells with the emulsion phase, cell-laden microcapsules with uniform size could be generated by electrospray (Fig. S4). Human gallbladder cancer cells (SGC-996) were encapsulated in the hybrid microcapsules with a density of 2.5×10^5 cells mL^{-1} and cultured in the complete H-DMEM for 24 days (Fig. 5a). It can be observed that cells gradually aggregate into clusters and then grew into tumor spheroids. After culture for 24 days, the cell viability in the capsule was examined by a live/dead assay. Relatively large tumor spheroids with diameters ranging from 200 to 300 μm can be found in capsules, suggesting the good permeability and cytocompatibility of the capsules (Fig. 5b-d). As a comparative study, GBC cells were encapsulated in the alginate microparticles. With sufficiently long-time of *in-vitro* culture, the cell spheroids cultured in microparticles are relatively small, with an average size of less than 150 μm (Fig. 5e). Cell viability test shows that both capsules and particles have a good cytocompatibility. The low permeability of solid hydrogel, in together with the retarded cell-to-cell contact may explain the differences in cell assembly and size of tumor spheroids.[39] Besides, capsules can physically entrap more cells than alginate particles, attributed to the PEGylated fibril cluster that inhibit protein adsorption and cell adhesion.

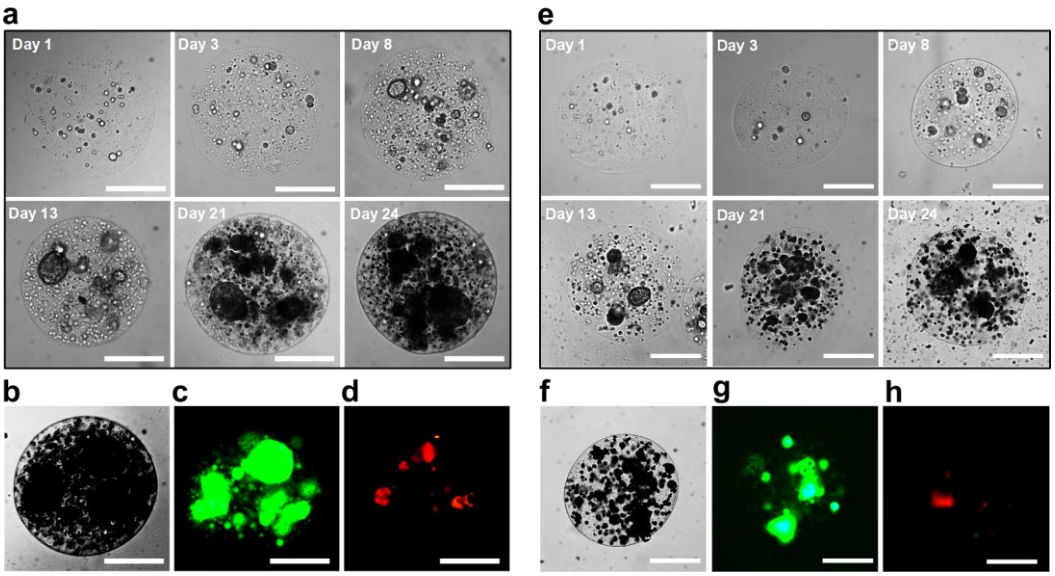

Fig. 6 Representative images of SGC-996 cell spheroids after encapsulation in (a) microcapsules and (e) alginate hydrogel particles for 1, 3, 8, 13, 21, and 24 days. The cell viability of cell spheroids in (b-d) microcapsules and (f-h) alginate hydrogel particles evaluated at day 24 by Live/Dead staining. The green and red fluorescence represent live and dead cells, respectively. Scale bars: 250 μm.

Conclusions

In conclusion, we develop an all-aqueous microfluidic approach to fabricate robust protein capsules by using fibril clusters adsorbed at the water/water interface. We show that fibril cluster better stabilize W/W emulsion than simple fibrils, and robust capsules can be prepared by complexing the fibril cluster and alginate at the W/W interface. This mild approach enables encapsulation of living cells and culture of large tumor spheroids *in vitro*, with great potentials to be used for cancer drug screening or 3D printing of living tissue in hydrogel-free all-aqueous multiphase environment.

Experimental Section

Materials: Dextran (500 kDa, Macklin), PEG (35 kDa, Sigma), hen egg white lysozyme (Macklin), star-shaped 4-arm maleimido-poly(ethylene glycol) ($(MAL)_4$-PEG, 2 kDa, 5 kDa, 10 kDa, Seebio Biotech), maleimide-PEG-methoxy (MAL-PEG, 2 kDa, Seebio Biotech), furfurylamine (Macklin), 4-(4,6-dimethoxy-1,3,5-triazin-2-yl)-4-methylmorpholinium chloride (DMTMM, Macklin), alginate (BR, Aladdin), thioflavine T (ThT, Aladdin), FITC-dextran (150 kDa, 2000 kDa, STANDARDS). All other reagents were purchased from Aladdin and were analytical grade.

Synthesis of protein fibrils (PF) and furan-fibril/$(MAL)_4$-PEG clusters. A 20 mg/mL solution of lysozyme was prepared by dissolving 0.2 g of protein into 60 mL of solution containing 12 mL of 1 M HCl, 36 ml of 10 mM HCl and 12 ml of 10 mM NaCl. To induce fibril formation, the solution was incubated at 75 °C and stirred at 550 rpm for 65 h.[17] Subsequently, furfurylamine modified fibril was prepared by using the amidation reaction following the protocol according to Cai et al.[40] In a typical experiment, DMTMM (1.4 g) was added into the fibril suspension (2.0%, w/v, 50 mL) and kept stirring for 20 min to fully activate the carboxyl groups of fibril. Then, furfurylamine (0.75 g) was added dropwise to the suspension. This reaction was maintained at room temperature for 24 h under continuous stirring. Afterwards, furan-fibril was cross-linked using $(MAL)_4$-PEG via D−A click chemistry. In a representative example, an appropriate amount of $(MAL)_4$-PEG was added into the furan-fibril suspension and allowed to react overnight at room temperature to give the fibril clusters. For fibril clusters synthesized by $(MAL)_4$-PEG with different average molecular

weights (Mw, 2 kDa, 5 kDa, and 10 kDa), the products were named as PF-2k, PF-5k, and PF-10k. For fibril clusters synthesized by $(MAL)_4$-PEG (10 kDa) at different reactant ratios (the amount of $(MAL)_4$-PEG added into 200 μL furan-fibril suspension was 0.05 g, 0.10 g, 0.15 g, and 0.20 g), the products were named as PF-1, PF-2, PF-3, and PF-4, respectively. 1-arm MAL-PEG (0.16 g) was also used to graft onto the furan-fibril (200 μL furan-fibril suspension) for comparative study.

FT-IR characterization. Fibril, furan-fibril and fibril cluster (PF-4) were dialyzed against ultrapure water for 4 days at room temperature. The purified samples were finally freeze-dried. The changes in the chemical structure of dried fibril, furan-fibril and fibril cluster samples, as well as $(MAL)_4$-PEG (10 kDa) were qualitatively analyzed using FT-IR (Spectrum 100, Perkin Elmer, Inc., USA). Samples were prepared by grinding the finely powdered samples with potassium bromide (KBr) and pressed into tablets. The spectrum was recorded over the wavenumber range of 4000-400 cm^{-1}.

Particle size and zeta potential measurements. A Zetasizer Nano-ZS90 (Malvern) was employed to measure the particle size and zeta potential of the fibril and fibril cluster suspensions. The measurements were taken immediately after diluting the samples to 0.02% (w/v, counted by fibrils) with NaCl solution (0.9%). All measurements were performed in triplicate at 25 °C.

Characterization of emulsion stability and partitioning of fibrils or fibril clusters. A total of 3% (w/v) dextran and 7% (w/v) PEG were dissolved into a 0.05-0.15% (w/v, counted by fibrils) fibril or fibril cluster suspensions, which was diluted by ultrapure water or high glucose Dulbecco's Modified Eagle Medium (H-DMEM, Gibco)

supplemented with 10% fetal bovine serum (FBS, Gibco) and 1% penicillin/streptomycin (Gibco). A vortex was employed to prepare the emulsions and ThT (2 mM) was used to label the fibrils or clusters. For dextran/PEG emulsions in water, the pH of the system was adjusted to neutral pH using HCl. The emulsion stability was monitored after vortexing for 2 min under a fluorescence microscope (LWD300-38HMC, CEWEI). The fibril or fibril cluster partitioning in the emulsions were imaged. A blue laser with a maximum excitation wavelength of 445 nm was used to excite and detect the ThT-labelled fibrils or clusters. Besides, the fibril or cluster partitioning in emulsions were also characterized by a confocal laser scanning microscope (CLSM, Leica TCS SP8 STED 3X). Moreover, another method was used to characterize the partitioning of fibrils or clusters in two phases. Initially, the fibrils and clusters in the suspensions were labelled with ThT and incubated at 60 °C for 15 min. Then the samples were washed using PBS through centrifugation (15000 rpm, 8 min) for 3 times to remove the free ThT. Subsequently, a 15% (w/v) dextran solution and an 8% (w/v) PEG solution in PBS were mixed at a 1:1 volume ratio, and the fibrils or clusters labelled with ThT were added to the mixture. After homogeneous mixing, the mixtures were centrifugated (800 rpm, 10 min) and gingerly transferred to the transparent sample cells. The partitioning of yellow fibrils or clusters can be observed by naked eyes.

Fabrication of microcapsules. To prepare microcapsules with uniform size, the electrospray approach was employed to produce W/W emulsion droplets firstly. An emulsion phase containing 10% (w/v) dextran and 0.3% (w/v) alginate was

electrosprayed in air to form droplets, and the emulsion phase was dissolved in the complete H-DMEM medium. The applied voltage was 2.2~2.4 kV and the distance between the anodic nozzle and cathode was 1.5 mm. The droplets were collected in a petri dish containing 3 ml PEG-rich continuous phase (8% PEG, 0.02% PF-4, and 0.1% pluronic@-127, w/v) and placed at room temperature for 1 h. Then, 3 ml of 0.2% (w/v) $CaCl_2$/8% (w/v) PEG solution was slowly injected into the petri dish. Both of the continuous phase and the $CaCl_2$/PEG solution was dissolved in the normal saline.

Morphological analysis of fibrils, fibril clusters and microcapsules. To preserve the original morphology, the microcapsules were first immobilized in 4% glutaraldehyde for 1 h, followed by pure water wash for several times. Subsequently, the dehydration was carried out through an ethanol gradient (25%, 50%, 75%, and 100%) for 10 min each and then dried in the vacuum oven or the liquid carbon dioxide at its super critical point. The PF and PF-4 samples were dehydrated by an ethanol gradient and dried in the liquid carbon dioxide at its super critical point. The immobilized microcapsules, PF and PF-4 samples were coated with a thin film of gold and observed under SEM (JSM-7800F, 5 kV).

Decomposition of microcapsules. The decomposition of microcapsules by using sodium citrate and trypsin-EDTA were investigated. Microcapsules encapsulating FITC-dextran (Mw: 2000 kDa) were treated by sodium citrate (150 mM) and trypsin-EDTA (0.25% and 0.125%, w/v) for different time, separately. During treating, the release of FITC-dextran and the morphological evolution of capsules were monitored and imaged.

Characterization of the microcapsules' permeability and mechanical properties. FITC-dextran with different Mw (150 and 2000 kDa) were mixed with the emulsion phase at a concentration of 0.03% (w/v). Microcapsules were prepared using the previously described method using this solution. For expansion and release studies, a microcapsule was initially transferred into an isotonic 15% (w/v) dextran solution dissolved in the normal saline. A certain amount (20~50 μL) of the solution in external phase was slowly replaced by normal saline with the same volume using the pipette, and then placed for over 10 min to make the expansion of microcapsule reach equilibrium and imaged using the fluorescence microscope. At the same time, the release of FITC-dextran was monitored. The operation was repeated until the final concentration of dextran in external phase less than 1% (w/v). The diameters of the microcapsules at different stages were measured using ImageJ image analysis software (NIH, USA).

Besides the single-capsule measurements, an ensemble method-rheology was also used to determine the mechanical properties of microcapsules. Different amounts of microcapsules were produced and gingerly transferred into a 15% (w/v) dextran solution dissolved in the normal saline to avoid microcapsule sedimentation during rheology measurements. The final volume fractions of microcapsule suspensions were 10% (v/v) and 40% (v/v), and pure dextran solution was used as a control sample. All rheological measurements were performed on a stress-controlled rheometer (Haake, MARS III, Thermo Fisher, USA) using concentric cylinder geometry with a bob diameter of 25.960 mm and a cup diameter of 27.200 mm. Dynamic frequency sweeps

were conducted at 25 °C and an strain amplitude of $\gamma_0 = 1\%$. This strain was confirmed by a dynamic strain sweep to be in the linear viscoelastic regime for all microcapsule suspensions. Then steady shear measurements were conducted at 25 °C. Sample evaporation was minimal in this geometry because of the small area exposed to the atmosphere relative to the volume of the sample.

Cell culture. Human Gallbladder carcinoma (GBC) cell line SGC-996 was purchased from the Cell Bank of the Chinese Academy of Science (Shanghai, China). The cells were cultured in complete H-DMEM medium in a humidified atmosphere with 5% CO_2 at 37 °C. Cells were digested with 0.25% (w/v) trypsin−EDTA (Sigma) for 2 min and centrifuged at 1200 rpm for 5 min.

Generation of cell-laden microcapsules and alginate hydrogel microparticles, 3D cell culture and cell's viability of encapsulated cells. Prior to the electrospraying, the cells were digested and suspended in emulsion phase containing 10% (w/v) dextran and 0.3% (w/v) alginate at a cell density of 2.5×10^5 cells mL^{-1}. Cell-laden microcapsules were then generated using the aforementioned method. For the fabrication of cell-laden microparticles, the emulsion phase contained 10% (w/v) dextran and 0.5% (w/v) alginate at a cell density of 2.5×10^5 cells mL^{-1}, and the continuous phase contained 8% PEG, 1.5% $CaCl_2$, and 0.1% pluronic@-127 (w/v). Then the continuous phase was washed 3 times using the normal saline, followed by the culture medium. The cell-laden microcapsules or microparticles were cultured in the H-DMEM containing 10% FBS and 5% penicillin/streptomycin in the incubator. Cell culture medium was changed every 10 days. During 24 days of 3D culture, the cell-laden microcapsules or

microparticles were observed and imaged at days 1, 3, 8, 13, 21 and 24 using a microscope to record the morphology change. Cell viability of encapsulated cells was evaluated by using live/dead assay. The cell-laden microcapsules or microparticles were incubated in cell culture medium with calcein AM (green, live, 1:1000) and propidium iodide (red, dead, 1:1000) (LIVE/DEAD viability/cytotoxicity assay kit, Gibco) at 37 °C for 30 min. Then, the samples were imaged under a fluorescence microscope (DMi8, Leica Microsystems GmbH, Germany).

Acknowledgements

This work was supported by the National Natural Science Foundation of China (52203121), and the China Postdoctoral Science Foundation (2021M692211, 2020M681308, 2020T130411).

References

1. Chao, Y.; Shum, H. C., Emerging aqueous two-phase systems: from fundamentals of interfaces to biomedical applications. *Chemical Society Reviews* **2020,** *49* (1), 114-142.

2. Zhao, H.; Ibrahimova, V.; Garanger, E.; Lecommandoux, S., Dynamic Spatial Formation and Distribution of Intrinsically Disordered Protein Droplets in Macromolecularly Crowded Protocells. *Angewandte Chemie International Edition* **2020,** *59* (27), 11028-11036.

3. Sabari, B. R.; Dall'Agnese, A.; Boija, A.; Klein, I. A.; Coffey, E. L.; Shrinivas, K.; Abraham, B. J.; Hannett, N. M.; Zamudio, A. V.; Manteiga, J. C.; Li, C. H.; Guo, Y. E.;

Day, D. S.; Schuijers, J.; Vasile, E.; Malik, S.; Hnisz, D.; Lee, T. I.; Cisse, I. I.; Roeder, R. G.; Sharp, P. A.; Chakraborty, A. K.; Young, R. A., Coactivator condensation at super-enhancers links phase separation and gene control. *Science* **2018,** *361* (6400), eaar3958.

4. Ma, Q.; Song, Y.; Sun, W.; Cao, J.; Yuan, H.; Wang, X.; Sun, Y.; Shum, H. C., Cell-Inspired All-Aqueous Microfluidics: From Intracellular Liquid–Liquid Phase Separation toward Advanced Biomaterials. *Advanced Science* **2020,** *7* (7), 1903359.

5. Daradmare, S.; Lee, C.-S., Recent progress in the synthesis of all-aqueous two-phase droplets using microfluidic approaches. *Colloids and Surfaces B: Biointerfaces* **2022,** *219*, 112795.

6. Dewey, D. C.; Strulson, C. A.; Cacace, D. N.; Bevilacqua, P. C.; Keating, C. D., Bioreactor droplets from liposome-stabilized all-aqueous emulsions. *Nature Communications* **2014,** *5* (1), 4670.

7. Wang, C.; Zhang, Z.; Wang, Q.; Wang, J.; Shang, L., Aqueous two-phase emulsions toward biologically relevant applications. *Trends in Chemistry* **2023,** *5* (1), 61-75.

8. Vilabril, S.; Nadine, S.; Neves, C. M. S. S.; Correia, C. R.; Freire, M. G.; Coutinho, J. A. P.; Oliveira, M. B.; Mano, J. F., One-Step All-Aqueous Interfacial Assembly of Robust Membranes for Long-Term Encapsulation and Culture of Adherent Stem/Stromal Cells. *Advanced Healthcare Materials* **2021,** *10* (10), 2100266.

9. Wang, H.; Liu, H.; Zhang, X.; Wang, Y.; Zhao, M.; Chen, W.; Qin, J., One-Step Generation of Aqueous-Droplet-Filled Hydrogel Fibers as Organoid Carriers Using an All-in-Water Microfluidic System. *ACS Applied Materials & Interfaces* **2021,** *13* (2), 3199-3208.

10. Liu, H.; Wang, Y.; Wang, H.; Zhao, M.; Tao, T.; Zhang, X.; Qin, J., A Droplet Microfluidic System to Fabricate Hybrid Capsules Enabling Stem Cell Organoid Engineering. *Advanced Science* **2020,** *7* (11), 1903739.

11. Ying, G.-L.; Jiang, N.; Maharjan, S.; Yin, Y.-X.; Chai, R.-R.; Cao, X.; Yang, J.-Z.; Miri, A. K.; Hassan, S.; Zhang, Y. S., Aqueous Two-Phase Emulsion Bioink-Enabled 3D Bioprinting of Porous Hydrogels. *Advanced Materials* **2018,** *30* (50), 1805460.

12. Luo, G.; Yu, Y.; Yuan, Y.; Chen, X.; Liu, Z.; Kong, T., Freeform, Reconfigurable

Embedded Printing of All-Aqueous 3D Architectures. *Advanced Materials* **2019,** *31* (49), 1904631.

13. Zhang, S.; Qi, C.; Zhang, W.; Zhou, H.; Wu, N.; Yang, M.; Meng, S.; Liu, Z.; Kong, T., In Situ Endothelialization of Free-Form 3D Network of Interconnected Tubular Channels via Interfacial Coacervation by Aqueous-in-Aqueous Embedded Bioprinting. *Advanced Materials* **2022,** *n/a* (n/a), 2209263.

14. Qu, F.; Guilak, F.; Mauck, R. L., Cell migration: implications for repair and regeneration in joint disease. *Nature Reviews Rheumatology* **2019,** *15* (3), 167-179.

15. Silva, A. K. A.; Richard, C.; Bessodes, M.; Scherman, D.; Merten, O.-W., Growth Factor Delivery Approaches in Hydrogels. *Biomacromolecules* **2009,** *10* (1), 9-18.

16. Kim, T. G.; Shin, H.; Lim, D. W., Biomimetic Scaffolds for Tissue Engineering. *Advanced Functional Materials* **2012,** *22* (12), 2446-2468.

17. Song, Y.; Shimanovich, U.; Michaels, T. C. T.; Ma, Q.; Li, J.; Knowles, T. P. J.; Shum, H. C., Fabrication of fibrillosomes from droplets stabilized by protein nanofibrils at all-aqueous interfaces. *Nature Communications* **2016,** *7* (1), 12934.

18. Dupont, H.; Maingret, V.; Schmitt, V.; Héroguez, V., New Insights into the Formulation and Polymerization of Pickering Emulsions Stabilized by Natural Organic Particles. *Macromolecules* **2021,** *54* (11), 4945-4970.

19. Poortinga, A. T., Microcapsules from Self-Assembled Colloidal Particles Using Aqueous Phase-Separated Polymer Solutions. *Langmuir* **2008,** *24* (5), 1644-1647.

20. Qian, X.; Peng, G.; Ge, L.; Wu, D., Water-in-water Pickering emulsions stabilized by the starch nanocrystals with various surface modifications. *Journal of Colloid and Interface Science* **2022,** *607*, 1613-1624.

21. Binks, B. P.; Shi, H., Phase Inversion of Silica Particle-Stabilized Water-in-Water Emulsions. *Langmuir* **2019,** *35* (11), 4046-4057.

22. Ma, Q.; Song, Y.; Kim, J. W.; Choi, H. S.; Shum, H. C., Affinity Partitioning-Induced Self-Assembly in Aqueous Two-Phase Systems: Templating for Polyelectrolyte Microcapsules. *ACS Macro Letters* **2016,** *5* (6), 666-670.

23. Ma, Q.; Yuan, H.; Song, Y.; Chao, Y.; Mak, S. Y.; Shum, H. C., Partitioning-dependent conversion of polyelectrolyte assemblies in an aqueous two-phase system.

Soft Matter **2018,** *14* (9), 1552-1558.

24. Buzza, D. M. A.; Fletcher, P. D. I.; Georgiou, T. K.; Ghasdian, N., Water-in-Water Emulsions Based on Incompatible Polymers and Stabilized by Triblock Copolymers–Templated Polymersomes. *Langmuir* **2013,** *29* (48), 14804-14814.

25. Antipov, A. A.; Sukhorukov, G. B., Polyelectrolyte multilayer capsules as vehicles with tunable permeability. *Advances in Colloid and Interface Science* **2004,** *111* (1), 49-61.

26. Chen, T.; Wang, Y.; Xie, J.; Qu, X.; Liu, C., Lysozyme Amyloid Fibril-Integrated PEG Injectable Hydrogel Adhesive with Improved Antiswelling and Antibacterial Capabilities. *Biomacromolecules* **2022,** *23* (3), 1376-1391.

27. Gustafsson, L.; Tasiopoulos, C. P.; Jansson, R.; Kvick, M.; Duursma, T.; Gasser, T. C.; van der Wijngaart, W.; Hedhammar, M., Recombinant Spider Silk Forms Tough and Elastic Nanomembranes that are Protein-Permeable and Support Cell Attachment and Growth. *Advanced Functional Materials* **2020,** *30* (40), 2002982.

28. Das, S.; Jacob, R. S.; Patel, K.; Singh, N.; Maji, S. K., Amyloid Fibrils: Versatile Biomaterials for Cell Adhesion and Tissue Engineering Applications. *Biomacromolecules* **2018,** *19* (6), 1826-1839.

29. Shuai, Y.; Mao, C.; Yang, M., Protein Nanofibril Assemblies Templated by Graphene Oxide Nanosheets Accelerate Early Cell Adhesion and Induce Osteogenic Differentiation of Human Mesenchymal Stem Cells. *ACS Applied Materials & Interfaces* **2018,** *10* (38), 31988-31997.

30. Li, S.; Yi, J.; Yu, X.; Shi, H.; Zhu, J.; Wang, L., Preparation and Characterization of Acid Resistant Double Cross-Linked Hydrogel for Potential Biomedical Applications. *ACS Biomaterials Science & Engineering* **2018,** *4* (3), 872-883.

31. Nimmo, C. M.; Owen, S. C.; Shoichet, M. S., Diels−Alder Click Cross-Linked Hyaluronic Acid Hydrogels for Tissue Engineering. *Biomacromolecules* **2011,** *12* (3), 824-830.

32. Harada, A.; Kimura, Y.; Kojima, C.; Kono, K., Effective Tolerance to Serum Proteins of Head−Tail Type Polycation Vectors by PEGylation at the Periphery of the Head Block. *Biomacromolecules* **2010,** *11* (4), 1036-1042.

33. He, Q.; Zhang, J.; Shi, J.; Zhu, Z.; Zhang, L.; Bu, W.; Guo, L.; Chen, Y., The effect of PEGylation of mesoporous silica nanoparticles on nonspecific binding of serum proteins and cellular responses. *Biomaterials* **2010,** *31* (6), 1085-1092.

34. Allain, C.; Cloitre, M., Interaction between Particles Trapped at Fluid Interfaces: II. Free-Energy Analysis of the Interaction between Two Horizontal Cylinders. *Journal of Colloid and Interface Science* **1993,** *157* (2), 269-277.

35. Lahooti, S.; Sefton, M. V., Effect of an immobilization matrix and capsule membrane permeability on the viability of encapsulated HEK cells. *Biomaterials* **2000,** *21* (10), 987-995.

36. Larson, R. G., *The structure and rheology of complex fluid*. Oxford University Press: New York, 1999.

37. Dhand, A. P.; Poling-Skutvik, R.; Osuji, C. O., Simple production of cellulose nanofibril microcapsules and the rheology of their suspensions. *Soft Matter* **2021,** *17* (17), 4517-4524.

38. Zhu, K.; Yu, Y.; Cheng, Y.; Tian, C.; Zhao, G.; Zhao, Y., All-Aqueous-Phase Microfluidics for Cell Encapsulation. *ACS Applied Materials & Interfaces* **2019,** *11* (5), 4826-4832.

39. Qazi, T. H.; Mooney, D. J.; Duda, G. N.; Geissler, S., Biomaterials that promote cell-cell interactions enhance the paracrine function of MSCs. *Biomaterials* **2017,** *140*, 103-114.

40. Cai, Z.; Hu, S.; Wei, Y.; Huang, T.; Yu, A.; Zhang, H., In Situ Room-Temperature Cross-Linked Highly Branched Biopolymeric Binder Based on the Diels–Alder Reaction for High-Performance Silicon Anodes in Lithium-Ion Batteries. *ACS Applied Materials & Interfaces* **2021,** *13* (47), 56095-56108.